A Theoretically Rigorous Full-Wave Finite-Element-Based Solution of Maxwell's Equations From dc to High Frequencies

Jianfang Zhu, *Student Member, IEEE*, and Dan Jiao, *Senior Member, IEEE*

***Abstract*—It has been observed that finite element based solutions of full-wave Maxwell's equations break down at low frequencies. In this paper, we present a theoretically rigorous method to fundamentally eliminate the low-frequency breakdown problem. The key idea of this method is that the original *frequency-dependent* deterministic problem can be rigorously solved from a generalized eigenvalue problem that is *frequency independent*. In addition, we found that the zero eigenvalues of the generalized eigenvalue problem cannot be obtained as zeros because of finite machine precision. We hence correct the inexact zero eigenvalues to be exact zeros. The validity and accuracy of the proposed method have been demonstrated by the analysis of both lossless and lossy problems having on-chip circuit dimensions from dc to high frequencies. The proposed method is applicable to any frequency. Hence it constitutes a universal solution of Maxwell's equations in a full electromagnetic spectrum. The proposed method can be used to not only fundamentally eliminate the low-frequency breakdown problem, but also benchmark the accuracy of existing electromagnetic solvers at low frequencies including static solvers. Such a benchmark does not exist yet because full-wave solvers break down while static solvers involve theoretical approximations.**

***Index Terms*—Electromagnetic analysis, finite element methods, full-wave analysis, low-frequency breakdown, very large scale integrated (VLSI) circuits.**

I. Introduction

THE finite-element method (FEM) has been widely used for electromagnetic analysis due to its great capability in handling arbitrary inhomogeneous materials and irregularly shaped structures. In recent years, the method has been used for the design and analysis of very large scale integrated (VLSI) circuits because process scaling and frequency scaling necessitate a full-wave based analysis [1]–[3]. However, it has been found that a full-wave FEM-based solver, i.e., an FEM-based solution of full-wave Maxwell's equations, breaks down at low frequencies [4]–[9]. The typical breakdown frequency is tens of megahertz in VLSI circuit applications, which falls right into the frequency range in which a VLSI circuit works. Thus, the low-frequency breakdown problem becomes a very critical problem that demands an effective solution. The low-frequency breakdown problem has also been observed in integral-equation based solvers [10]–[14].

In order to overcome the low-frequency breakdown problem, a natural solution is to stitch a static- or quasistatic-based electromagnetic solver with a full-wave-based electromagnetic solver. However, this solution is cumbersome and inaccurate. First, one has to develop and accommodate both tools and switch between these two when necessary. More importantly, at which frequency such a switching is necessary is questionable. The starting frequency point at which a full-wave solution breaks down is different for different problems. For simple structures, given a frequency, designers can still use their physical intuitions to judge whether the breakdown occurs or not; for complicated circuits, however, it is difficult to make such judgment. Third, static or quasi-static solvers by themselves involve theoretical approximations because they assume that $\mathbf{E}$ and $\mathbf{H}$ are decoupled at low frequencies. However, in Maxwell's equations, $\mathbf{E}$ and $\mathbf{H}$ are always coupled as long as frequency is not zero. Although static solvers have been successful at low frequencies in practical applications, one also has to admit the fact that they are not theoretically rigorous. Decoupling $\mathbf{E}$ and $\mathbf{H}$ can result in a different level of accuracy at different frequencies.

The other popular solution to the low-frequency breakdown problem is to switch basis functions. For example, the loop-tree and loop-star basis functions [10], [12] were used to achieve a natural Helmholtz decomposition of the current to overcome the low-frequency breakdown problem in integral-equation-based methods. As another example, the tree-cotree splitting scheme [5], [6] was used to provide an approximate Helmholtz decomposition for edge elements in finite-element-based methods. The edge basis functions were used on the cotree edges, whereas the scalar basis functions were incorporated on the free nodes associated with the tree edges to represent the gradient field. Again, this solution is not convenient since one has to change basis functions, and hence the system matrix, to extend the applicability of a full-wave solver to low frequencies. In addition, the same approach can not be applied to high frequencies. In other words, the solution is not universal across all frequencies. Moreover, Helmholtz decomposition of the field by itself is not theoretically rigorous since it is exact only at dc. In addition, existing tree-cotree splitting based FEM solutions of vector wave equa-

Manuscript received January 30, 2010; revised May 27, 2010; accepted June 27, 2010. Date of publication August 09, 2010; date of current version January 07, 2011. This work was supported in part by a grant from Intel Corporation, in part by the National Science Foundation under Award 0747578, and in part by the Office of Naval Research under Award N00014-10-1-0482. This work was recommended for publication by Associate Editor J. Tan upon evaluation of the reviewers comments.

The authors are with the School of Electrical and Computer Engineering, Purdue University, West Lafayette, IN 47907 USA.

Color versions of one or more of the figures in this paper are available online at http://ieeexplore.ieee.org.

Digital Object Identifier 10.1109/TADVP.2010.2057428

tions have not fundamentally solved the low-frequency breakdown problem. For example, it was shown that a tree-cotree splitting scheme can be used to extend a full-wave finite-element-based solution to 1 MHz for typical on-chip dimensions [6]. However, for frequencies lower than 1 MHz, extrapolation techniques are required.

In [8], we developed a solution in the framework of a 2.5-D eigenvalue-based FEM method for the modeling of on-chip interconnects from dc to high frequencies. In [9], we developed a method to eliminate the low-frequency breakdown problem for the 3-D FEM-based solution of vector wave equations. Both solutions have two important advantages. First, they avoid switching basis functions. The same system matrix is used across all frequencies. Second, the solutions are valid at frequencies as low as dc. With the two advantages achieved, the solutions can be incorporated into any existing FEM solver to remove the low-frequency problem with great ease. The solutions developed in [8] and [9] both have an underlying assumption that at low frequencies where a full-wave solution breaks down, $\mathbf{E}$ and $\mathbf{H}$ are decoupled. While they continue to be effective and efficient in practical applications, in this work, we aim to develop a theoretically rigorous approach that does not require such a static assumption.

There are two reasons for us to consider a theoretically rigorous approach to solving Maxwell's coupled equations from dc to any high frequency. First, such an approach can be used to completely eliminate the low-frequency breakdown problem. Second, such an approach can be used as a golden reference to benchmark the accuracy of any electromagnetic solver at low frequencies. Such a golden reference in fact does not exist yet because full-wave solvers break down at low frequencies, while static solvers involve theoretical approximations. One might argue that the accuracy of an electromagnetic solver at low frequencies can always be tested out by checking the solution error using the relative residual. However, the system matrix resulting from a full-wave analysis at low frequencies has such a high condition number that a slight error in matrix solution can result in a big difference in the residual, and hence the relative residual cannot be used as a criterion to validate the electromagnetic solver at low frequencies. Certainly, there exist a few structures that have analytical solutions. However, for complicated structures, one still have to rely on a numerical solution that is theoretically rigorous to benchmark the accuracy.

In this work, we first perform a theoretical analysis of the low-frequency breakdown problem. We conclude that as long as computers have finite precision, the conventional FEM-based solution of full-wave Maxwell's equations would break down at certain frequency. This is true not only for VLSI circuits, but also for traditional millimeter and microwave circuits. The problem is not important in the latter because the breakdown frequency typically is out of the frequency range in which a millimeter or microwave circuit works. However, for the former, the breakdown problem is very significant because a full-wave solution breaks down at the working frequencies of a VLSI circuit.

Therefore, the question here is: given finite machine precision, how to bypass the low-frequency breakdown problem without decoupling $\mathbf{E}$ and $\mathbf{H}$? The proposed method is developed to answer this question. In this method, we rigorously transform the original *frequency-dependent* deterministic problem to a generalized eigenvalue problem that is *frequency independent*. From the solution of the generalized eigenvalue problem, we can use the modal superposition method [15]–[17] to rigorously obtain the solution of the original frequency dependent problem. Since the transformed eigenvalue problem does not depend on frequency, the low-frequency breakdown problem is naturally bypassed. However, this does not completely solve the problem because the zero eigenvalues of the resultant eigenvalue system due to either the null space of the stiffness matrix or the dc mode of the physical circuit cannot be obtained as exact zeros numerically. This is because the largest eigenvalue, i.e., the highest resonance frequency of a VLSI circuit, is extremely large due to micrometer level physical dimensions. And hence any eigenvalue that is 10^{-16} smaller than the largest eigenvalue is in fact zero in double precision computing. Thus, the problem of inexact zero eigenvalues can be fixed easily by correcting them to be zeros.

The proposed theoretically rigorous approach has the following important merits. 1) It does not involve any theoretical approximation. 2) It avoids switching basis functions. The edge basis that is traditionally used for vector finite element analysis is employed across all frequencies. 3) It preserves the system matrix. The same mass and stiffness matrices that are constructed in a traditional full-wave FEM solver are used from dc to high frequencies. 4) The approach is equally applicable to any high frequency in addition to low frequencies, and hence constituting a universal solution to Maxwell's equations in a full electromagnetic spectrum.

II. Analysis of the Low-Frequency Breakdown Problem

A. 3D Full-Wave Finite-Element-Based Solution

Consider the second-order vector wave equation

$$\nabla \times \left[\mu_r^{-1} \nabla \times \mathbf{E}\right] - \omega^2 \epsilon_r / c^2 \mathbf{E} = -j\omega\mu_0 \mathbf{J} \tag{1}$$

where μ_r is relative permeability, ϵ_r is relative permittivity, ω is angular frequency, c is the speed of light, and $\mathbf{J}$ represents a current source.

By expanding the unknown $\mathbf{E}$ using vector basis function $\mathbf{N}$ as

$$\mathbf{E} = \sum_{i=1}^{n} u_i \mathbf{N}_i \tag{2}$$

a finite-element-based analysis of (1) subject to the Dirichlet- or Neumann-type boundary condition yields the following matrix equation [18]:

$$(\mathbf{S} - \omega^2 \mathbf{T}) u = b \tag{3}$$

where $\mathbf{S}$ is known to be a stiffness matrix, $\mathbf{T}$ is known to be a mass matrix, and b is an excitation vector. The $\mathbf{S}$, $\mathbf{T}$, and b are assembled from their elemental contributions as follows:

$$\mathbf{S}_{ij}^{e} = \iiint_{V^e} (\nabla \times \mathbf{N}_i) \cdot (\nabla \times \mathbf{N}_j) dV$$
$$\mathbf{T}_{ij}^{e} = \mu\epsilon \iiint_{V^e} \mathbf{N}_i \cdot \mathbf{N}_j dV$$
$$b_i^e = -j\omega\mu \iiint_{V^e} \mathbf{N}_i \cdot \mathbf{J} dV. \quad (4)$$

In vector finite element analysis, the most widely used basis is the edge basis [18], [19].

It was shown by our numerical experiments that, in general, the solution of (3) breaks down at tens of megahertz in typical on-chip problems, the electric size of which can be smaller than 10^{-9} wavelengths. As an example, consider a 3-D on-chip interconnect, the cross-sectional view of which is shown in Fig. 1(a). The structure is of length 2000 μm into the paper. The interconnect involves a center strip line with two parallel return wires in M2 layer, a metal plane that is 0.2 μm thick in M1 layer, and a metal plane that is 1 μm thick in M3 layer. A current source is launched from the bottom plane to the center strip line. In Fig. 1(b), we plot the electric field distribution in the transverse plane at low frequencies, where each horizontal dashed line represents a material interface. Clearly, the FEM solution breaks down. Between M2 and M3, the electric field should point from the center strip to the upper metal plane, and be perpendicular to the upper metal plane, which cannot be seen from Fig. 1(b).

Equation (3) describes a lossless system. Consider a lossy system formed inside conductors. Note that at low frequencies, fields penetrate into conductors because skin depth can be comparable to or larger than the physical dimension of the conductor. In such a lossy system, the electric field $\mathbf{E}$ satisfies the following second-order vector wave equation:

$$\nabla \times \left[\mu_r^{-1} \nabla \times \mathbf{E}\right] - \omega^2 \epsilon_r / c^2 \mathbf{E} + j\omega\mu_0\sigma\mathbf{E} = -j\omega\mu_0 \mathbf{J} \quad (5)$$

where σ is conductivity. A finite element analysis of (5) *inside* good conductors results in the following system of equations:

$$(\mathbf{S} + j\omega\mathbf{R})u = b \quad (6)$$

where the mass matrix $\mathbf{T}$ is absent because inside a good conductor, displacement current can be ignored compared to conduction current. The loss-related matrix $\mathbf{R}$ has the following entries:

$$\mathbf{R}_{ij}^{e} = \mu\sigma \iiint_{V^e} \mathbf{N}_i \cdot \mathbf{N}_j dV. \quad (7)$$

At very low frequencies, we observe that the solution of (6) also breaks down, although the breakdown frequency is much lower than that of (3).

In the next section, we analyze the low-frequency breakdown problem, and show why the FEM-based solution of vector wave equations breaks down at low frequencies.

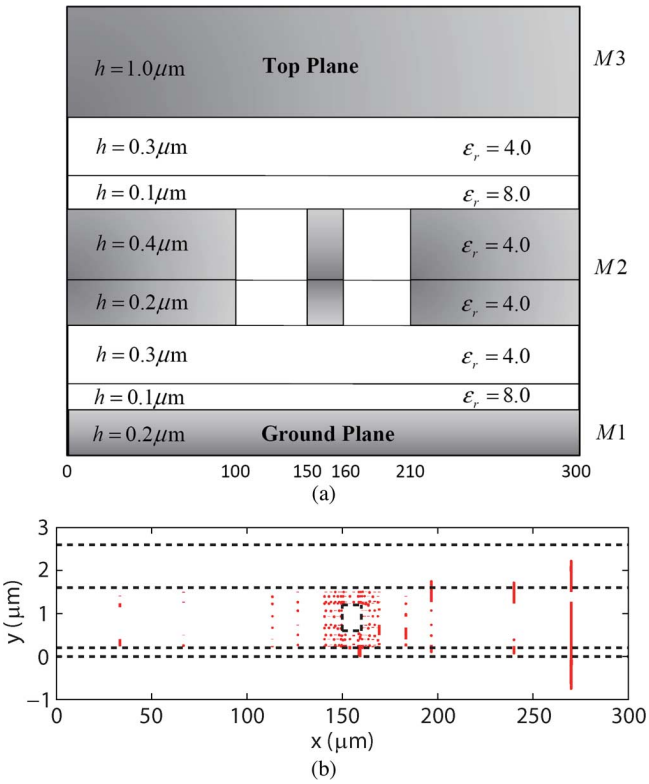

Fig. 1. (a) Cross-sectional view of a 3-D on-chip interconnect. (b) Electric field distribution generated by a conventional full-wave FEM-based analysis.

B. Analysis of Low-Frequency Breakdown Problem

To analyze the low-frequency breakdown problem, we examine the ratio of $\mathbf{S}$'s norm over $\mathbf{T}$'s norm in (3). From (4), it is clear that $\mathbf{S}_{ij}$ is an $O(l)$ quantity, and $\mathbf{T}_{ij}$ is a quantity proportional to $10^{-17}(l^3)$, where l is the average edge length in a 3-D discretization. Hence, we obtain the following relationship:

$$\frac{\|\mathbf{S}\|}{\|\mathbf{T}\|} = \frac{10^{17}}{O(l^2)} \quad (8)$$

where $\|.\|$ denotes a matrix norm. The above analysis is based on a normalized basis $\mathbf{N}$. If $\mathbf{N}$ is not normalized, although the norm of $\mathbf{T}$ and that of $\mathbf{S}$ change, the ratio of $\mathbf{S}$'s norm over $\mathbf{T}$'s norm remains the same as (8).

For circuits having large physical sizes such as millimeter wave circuits, l is in the order of 10^{-3} m. Hence the ratio of $\mathbf{S}$'s norm over $\mathbf{T}$'s norm is in the order of 10^{23}. However, for state-of-the-art VLSI circuits, l is at the level of 1 μm. Hence, the ratio of $\mathbf{S}$'s norm over $\mathbf{T}$'s norm is in the order of 10^{29}, which is significantly larger than that in a millimeter wave circuit.

Since $\|\mathbf{T}\|$ is 10^{-29} smaller than $\|\mathbf{S}\|$ in a VLSI circuit, at low frequencies, even one uses double-precision computing, the mass matrix $\mathbf{T}$ is essentially treated as zero by computers when performing the addition of $\mathbf{T}$ and $\mathbf{S}$. As a result, the breakdown occurs. If we directly solve (3) without scaling, we cannot preserve the effect of $\mathbf{T}$. However, if we scale $\mathbf{T}$, $\mathbf{S}$ has to be simultaneously scaled. Therefore, the bad scaling of (3) is caused by physics instead of numerical reasons. The large ratio between $\|\mathbf{S}\|$ and $\omega^2\|\mathbf{T}\|$ is dictated by the electric size of the structure,

which cannot be reduced by a matrix scaling technique. If an infinite-precision machine is available, the solution of (3) would not break down at low frequencies because the machine can capture the effect of $\mathbf{T}$.

For a lossy system shown in (6), the $\mathbf{R}_{ij}$ is a quantity proportional to $10^{-17}(l^3) \times \sigma/\epsilon$, and hence is much larger than $\mathbf{T}_{ij}$. As a result, the ratio of the $\mathbf{R}_{ij}$'s norm over $\mathbf{S}_{ij}$'s norm is much larger, and hence the breakdown frequency of (6) is much lower than that of a lossless system.

C. Identification of Breakdown Frequency

The above analysis also suggests an analytical way to estimate the breakdown frequency. As can be seen from (3), $\mathbf{T}$ is multiplied by ω^2 in the system matrix. Therefore, if the ratio of $||\mathbf{T}||$ over $||\mathbf{S}||$ is 10^{-29}, ω^2 has to be as large as $10^{13} - 10^{14}$ so that a double-precision computation can take $\mathbf{T}$'s contribution into consideration. Therefore, the breakdown frequency falls into the range of $10^6 - 10^7$ Hz for micrometer-scale structures, which shows excellent agreement with our numerical experiments.

For the lossy system formed inside a conductor, assuming σ is at the level of 10^7 S/m, then the ratio of $||\mathbf{R}||$ over $||\mathbf{S}||$ is $O(10^{-10})$. Hence, as long as ω^2 is no less than $10^{-5} - 10^{-6}$, the contribution of $\mathbf{R}$ can be effectively taken into consideration by double-precision computing. Therefore, the breakdown frequency for the lossy system formed inside a conductor falls into the range of $10^{-2} - 10^{-3}$ Hz for micrometer-scale structures, which also shows excellent agreement with our numerical experiments.

From the aforementioned analysis, it can be seen clearly that the low-frequency breakdown problem occurs earlier, i.e., at a higher frequency, in a lossless system than that occurs in a lossy system. In addition, due to finite machine precision, it is inevitable that the FEM based solution of vector wave equations break down at low frequencies. This breakdown occurs not only in VLSI circuits, but also in microwave and millimeter wave circuits, and other electromagnetic applications. For VLSI circuits and future nanometer circuit applications, the breakdown problem demands a solution because the breakdown frequency is within the working frequency band of the circuits, whereas the breakdown problem was ignored or may not be noticed in microwave applications because the breakdown frequency is so low that it is outside of the operating frequency band.

III. Proposed Theoretically Rigorous Solution

From Section II, apparently, as long as one solves coupled Maxwell's equations, and hence a combined $\mathbf{T}$ and $\mathbf{S}$ system like (3), one cannot fundamentally eliminate the low-frequency breakdown problem because computers have finite precision. Thus, employing static approximations such as decoupling $\mathbf{E}$ and $\mathbf{H}$ at low frequencies seems to be the only way forward. However, once one makes use of the static approximations, the resultant approach is not theoretically rigorous.

In the following, we propose a method that can fundamentally eliminate the low-frequency breakdown problem without making any theoretical approximation. In this method, we solve full-wave Maxwell's equations as they are without invoking static assumptions. We use the edge basis across frequencies from dc to high frequencies, and hence keeping the same mass and stiffness matrices throughout the frequencies. Our proposed solution is truly a unified solution from dc to any high frequency. This has not been achieved by existing methods developed for overcoming the low-frequency problem. For example, methods that rely on basis-function switching at low frequencies cannot apply the same basis function to high frequencies.

The key idea of the proposed method is that the *frequency dependent* deterministic problem in (3) can be rigorously solved by the following *frequency independent* eigenvalue problem [15]–[17]:

$$\mathbf{S}x = \lambda \mathbf{T}x \tag{9}$$

where λ is the eigenvalue, and x is the eigenvector. Since $\mathbf{S}$ is symmetric semi-positive definite and $\mathbf{T}$ is symmetric positive definite, the eigenvalues λ are non-negative real numbers. Meanwhile, the eigenvectors x are $\mathbf{S}$ and $\mathbf{T}$ orthogonal. Denoting the eigenvalues of (9) by $\lambda_1, \lambda_2, \cdots, \lambda_N$, and the corresponding eigenvectors by $x_1, x_2, \cdots, x_N$. Let $\Phi = [x_1, x_2, \cdots, x_N]$, we have

$$\begin{aligned} \Phi^T \mathbf{T} \Phi &= \mathbf{I} \\ \Phi^T \mathbf{S} \Phi &= \mathbf{\Lambda} \end{aligned} \tag{10}$$

where $\mathbf{I}$ is an identity matrix, and $\mathbf{\Lambda}$ is a diagonal matrix, the ith element of which is λ_i.

After solving the generalized eigenvalue problem (9), the deterministic problem (3) can be solved in the following way [15]–[17]. First, we expand unknown u of (3) in the space of Φ

$$u = \Phi \tilde{u} \tag{11}$$

where $\tilde{u}$ is an unknown coefficient vector, the element of which represents the weight of each eigen vector in u. Next, we solve for $\tilde{u}$.

Substituting (11) into (3), and testing (3) by Φ^T, we obtain

$$\Phi^T(\mathbf{S} - \omega^2 \mathbf{T})\Phi \tilde{u} = \Phi^T b. \tag{12}$$

Since Φ are $\mathbf{S}$ and $\mathbf{T}$ orthogonal as shown in (10), (12) becomes

$$\begin{pmatrix} \lambda_1 - \omega^2 & \cdots & 0 \\ \vdots & \ddots & \vdots \\ 0 & \cdots & \lambda_N - \omega^2 \end{pmatrix} \tilde{u} = \Phi^T b. \tag{13}$$

Thus, we can solve a diagonal system (13) to obtain $\tilde{u}$, from which u can be readily obtained from (11).

For a lossy system formed inside a conductor, we perform the same eigenvalue analysis (9) except that matrix T is replaced by R. We then substitute (11) into (6), and test (6) by Φ^T, we obtain

$$\Phi^T(\mathbf{S} + j\omega \mathbf{R})\Phi \tilde{u} = \Phi^T b. \tag{14}$$

Since Φ are $\mathbf{S}$ and $\mathbf{R}$ orthogonal, (14) again becomes a diagonal system

$$\begin{pmatrix} \lambda_1 + j\omega & \cdots & 0 \\ \vdots & \ddots & \vdots \\ 0 & \cdots & \lambda_N + j\omega \end{pmatrix} \tilde{u} = \Phi^T b \tag{15}$$

from which $\tilde{u}$ can be readily solved. Once $\tilde{u}$ is solved, u can be obtained from (11).

Clearly, the above solution that is based on modal superposition naturally bypasses the low-frequency breakdown problem, since (9) is frequency independent and (13) and (15) can be readily solved due to the diagonal nature of the system matrix. Equations (13) and (15) can be viewed as a number of decoupled 1×1 matrices. Even though the eigenvalue spectrum of (9) is very wide, resulting in a large condition number of (3), the diagonal nature of (13) and (15) makes the condition number of each 1×1 matrix equal to 1.

However the aforementioned modal superposition method for solving (3) and (6) does not completely solve the problem. We have to add another step after the eigenvalue solution. To explain, the eigenvalues of (9) can be divided into two groups. One group consists of all the zero eigenvalues associated with the null space of $\mathbf{S}$ as well as the physical dc modes of the structure such as an integrated circuit. The other group consists of the resonant frequencies of the 3-D structure being simulated. For VLSI circuits, the eigenvalues in the second group are extremely large because the geometrical dimensions of on-chip circuits are very small. For example, in a typical on-chip circuit having micrometers dimensions, the largest eigenvalue of (9) can be as large as 10^{30}. An eigenvalue solver generally converges to the maximum eigenvalue first, and hence the values that are sixteen orders of magnitude smaller than the maximum one are not distinguishable in double-precision computing. As a result, the zero eigenvalues of (9) are not found to be exact zeros numerically. Instead, for a structure having the largest eigenvalue 10^{30}, the zero eigenvalues of (9) are numerically obtained as 10^{14}. Furthermore, the smaller the physical dimension of the structure, the greater the largest eigenvalues, and hence the greater the eigenvalues which theoretically are zero but numerically are calculated to be nonzero.

When frequency is high, the inexact zero eigenvalues do not induce much error because $\lambda - \omega^2$ in (13) is still approximately equal to $-\omega^2$ even if λ is not exactly zero. However, at low frequencies, the error can be very significant. At a relatively low frequency, ω^2 can be easily overwhelmed by these inexact *zero* eigenvalues, leading to a completely wrong frequency dependence in the final solution u. Fortunately, even though the zero eigenvalues of (9) are not output as zeros by a computer due to finite precision, the eigenvectors of (9) are still accurate because they are $\mathbf{T}$ orthogonal, and hence in a similar order of magnitude. This can also be seen clearly from the following experiment. We solve the eigenvalue problem (9) from

$$\alpha \mathbf{S} x = \lambda \mathbf{T} x \tag{16}$$

where α is a scaling factor that is artificially introduced to normalize eigenvalues. Based on the ratio of $\mathbf{S}$'s norm over $\mathbf{T}$'s norm analyzed in Section II for typical on-chip circuits, α was chosen as 10^{-29}. The largest eigenvalue of (16) was found to be 10, whereas the smallest one, was found to be 10^{-16}, which is essentially zero. The eigenvectors of (16) are the same as those of (9), whereas the eigenvalues of (16) have to be multiplied by 10^{29} to obtain the eigenvalues of (9). Hence the 10^{-16} eigenvalue, which is a zero eigenvalue, becomes 10^{14} in (9). This proves why the 10^{14} eigenvalue of (9) is in fact zero, and why the eigenvectors are still correctly obtained.

A natural remedy to the inexact zero eigenvalue problem is as follows. After obtaining the eigenvalues of (9), we change all the eigenvalues which theoretically should be zero, but numerically obtained as nonzero, to be purely zero. Based on the fact that the generalized eigenvalue problem (9) is *scalable* with respect to length unit, the following approach can be used to identify zero eigenvalues without any difficulty.

Basically, the eigenvalues of (9) obtained from one length unit can be scaled to obtain the eigenvalues for another unit, while the eigenvectors remain the same. For example, given a structure the length unit of which is micrometer, one can compute (9) for the same structure but with *meter* being the unit, i.e., enlarging the geometrical dimension by 10^6. The resultant eigenvector x is the same as that of the original structure having micrometer unit, and the resultant eigenvalues scaled by 10^{12} are the same as the eigenvalues of the original structure. This is because matrix $\mathbf{S}$ is formed by the inner product of the *curl* of the vector basis functions, and matrix $\mathbf{T}$ is formed by the inner product of the vector basis functions, as shown in (4). In terms of length unit, the $\mathbf{S}$ is a quantity of $O(\mathrm{unit})$, whereas $\mathbf{T}$ is a quantity of $O(\mathrm{unit}^3)$, since the vector basis $\mathbf{N}$ is normalized. Therefore, the generalized eigenvalue problem (9) can be computed for a large unit, from which we can obtain the eigenvalues and eigenvectors for any other small unit. To be specific, assuming the real unit is w, after calculating (9) for a large unit v, we scale the eigenvalues λ by $(v/w)^2$ to obtain the true eigenvalues, while keeping the eigenvectors the same. The $(v/w)^2$ is essentially α in (16). With current machine precision, the zero eigenvalues of (9) for a large length unit can be computed as zeros accurately, thus there is no difficulty for a user of the proposed method to distinguish zero eigenvalues from nonzero ones.

Discussion: For null-space modes and dc modes of (9), we expect that $\mathbf{S}x = 0$ since the corresponding eigenvalues are zero. However, due to finite machine precision and extremely large resonant frequencies of on-chip circuits, the zero eigenvalues of (9) cannot be found as zero numerically. Instead, they are given by computers as large numbers in absolute values. This may mislead one to think that edge basis may have some problems at low frequencies. In fact, the $\mathbf{S}x$'s being nonzero for gradient-type modes is caused by finite machine precision.

One might argue that the proposed method of solving low-frequency breakdown problems is not practical because of the requirement of solving an eigenvalue problem. In fact, the proposed method is not only theoretically rigrous but also practical because at low frequencies, only a few eigenmodes need to be extracted as can be seen from (13), where the weight of the eigenmodes that have a nonzero eigenvalue λ_i is orders of magnitude smaller than that of the dc mode. Extracting a few selected eigenmodes out of (9) can be performed in linear complexity as can be seen from [3] and [20]. In addition, such an extraction only needs to be done once. It can be reused for all frequencies.

IV. Numerical Results

In order to verify the proposed method, first, a parallel-plate waveguide structure that has an analytical solution is simulated.

TABLE I
CAPACITANCE SIMULATED BY THE PROPOSED METHOD (C) AND CAPACITANCE SIMULATED BY THE TRADITIONAL FULL-WAVE FEM SOLVER (C^*)

Frequency (Hz)	C^* (pF)	C (pF)
1 K	-0.2758×10^{4}	3.0947×10^{-3}
1	-0.2758×10^{10}	3.0947×10^{-3}
10^{-32}	-0.2758×10^{72}	3.0947×10^{-3}

TABLE II
ELECTRIC FIELD SIMULATED BY THE PROPOSED METHOD ($\mathbf{E}$) AND ELECTRIC FIELD SIMULATED BY THE TRADITIONAL FULL-WAVE FEM SOLVER ($\mathbf{E}^*$)

Frequency (Hz)	$\|\|\tilde{\mathbf{E}}^*\|\|$ (V/m)	$\|\|\mathbf{E}\|\|$ (V/m)
1 K	1.38479×10^{12}	1.23429×10^{18}
1	1.38479×10^{9}	1.23429×10^{21}
10^{-32}	1.38479×10^{-23}	1.23429×10^{53}

The waveguide width, height, and length are set to be 10 μm, 1 μm, and 35 μm, respectively in accordance with the typical dimensions of on-chip circuits. The analytical capacitance is known for this structure, which is 3.0989×10^{-3} pF. A current source of 1 A is injected from the bottom plane to the top plane. The simulation based on a conventional full-wave FEM solver breaks down at 10 MHz, whereas the proposed solution is valid at all frequencies. In Table I, we compare the capacitance simulated using the proposed method and that simulated by a conventional FEM solver at 1 KHz, 1 Hz, and 10^{-32} Hz respectively. It is clear that the proposed solution agrees very well with the analytical solution, whereas the conventional FEM solver is totally wrong at low frequencies.

In addition, we compared the simulated electric field. At low frequencies, given a constant current, the voltage, and hence electric field is expected to scale with frequency as $O(\omega^{-1})$. This can also be seen from (13), at low frequencies, only zero eigenvalues are dominant. Since the right hand side b is linearly proportional to ω as can be seen from (4), $\tilde{u}$ in (13) should scale with frequency as $O(\omega^{-1})$, and hence u. In Table II, we compare the norm of the electric field $\mathbf{E}$ vector simulated by the proposed method and that of the conventional full-wave FEM solver. Clearly, the proposed method reveals an accurate frequency dependence in the field solution. In contrast, the traditional full-wave FEM solver gives a wrong frequency dependence.

In Fig. 2(a), we plot the electric field at each edge in the computational domain at 10^{-32} Hz simulated by the proposed method, which exhibits an open circuit phenomenon. Whereas, the traditional full-wave FEM solver gives very small magnitude, which is wrong, as shown in Fig. 2(b).

The proposed method is equally applicable at high frequencies without any modification. To validate it, we simulated the electric field of the parallel plate structure at three high frequency points: 10 GHz, 20 GHz, and 50 GHz respectively. In Table III, we list the norm of the electric field $\mathbf{E}$ vector simulated by the proposed method and that of the conventional full-wave FEM solver at the three frequencies. Clearly, the proposed method agrees very well with the conventional full-wave FEM solver at high frequencies.

Next we simulated the 3-D on-chip interconnect shown in Fig. 1(a). In this figure, the detailed geometrical and material

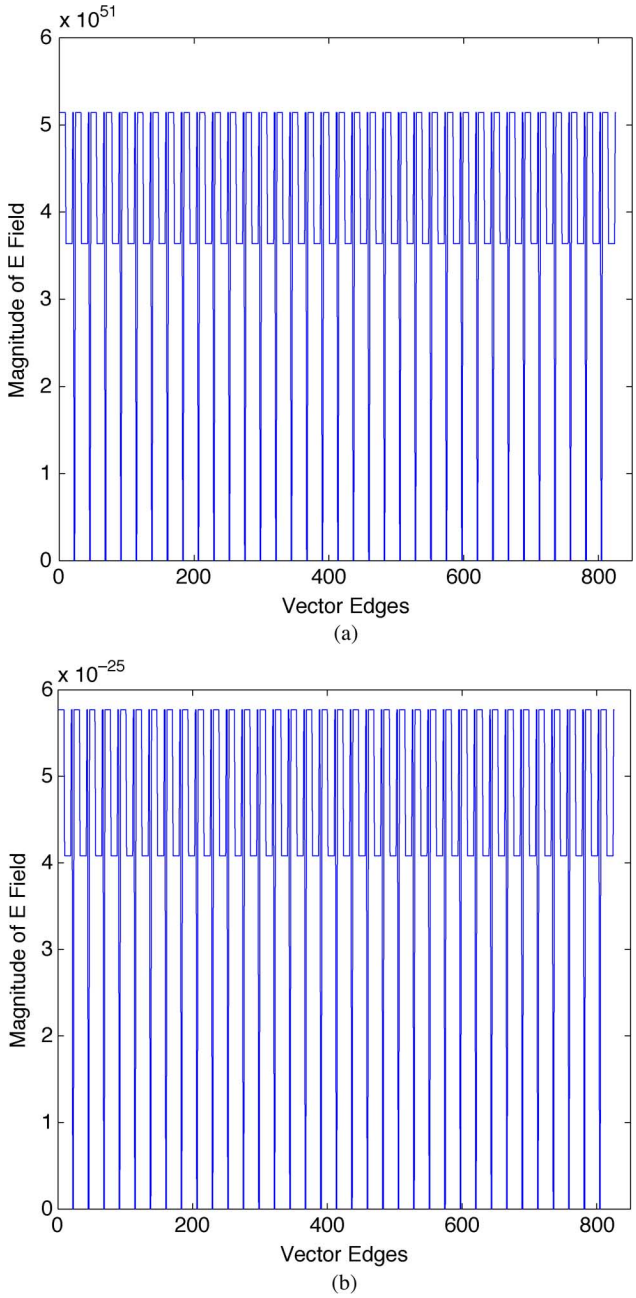

Fig. 2. Electric field simulated at each edge at 10^{-32} Hz. (a) Proposed method. (b) Traditional full-wave FEM solver.

TABLE III
ELECTRIC FIELD SIMULATED BY THE PROPOSED METHOD ($\mathbf{E}$) AND ELECTRIC FIELD SIMULATED BY THE TRADITIONAL FULL-WAVE FEM SOLVER ($\mathbf{E}^*$) AT HIGH FREQUENCIES

Frequency (Hz)	$\|\|\tilde{\mathbf{E}}^*\|\|$ (V/m)	$\|\|\mathbf{E}\|\|$ (V/m)
10 G	2.4686×10^{10}	2.4686×10^{10}
20 G	6.1714×10^{9}	6.1714×10^{9}
50 G	1.2343×10^{11}	1.2343×10^{11}

parameters are given. The structure is of length 2000 μm into the paper. Along the length direction, the front and the back end each is attached to an air layer, which is then truncated by a Neumann-type boundary condition. The top and bottom planes shown in Fig. 1(a) are backed by a perfect electric conducting

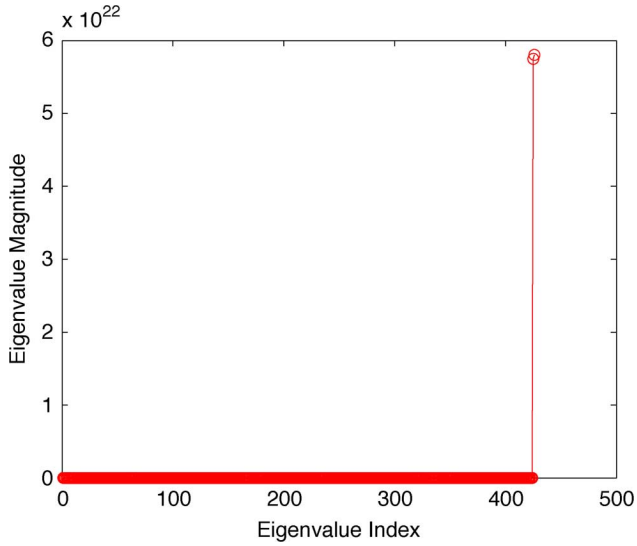

Fig. 3. The eigenvalues of a 3-D on-chip interconnect.

TABLE IV
EIGENVALUES OF A 3-D ON-CHIP INTERCONNECT

Index	Eigenvalue
420	1.0376E+16
421	1.08019E+16
422	1.1527E+16
423	1.43135E+16
424	8.26567E+16
425	5.75072E+22
426	5.80523E+22

(PEC) boundary condition. The left and right boundary conditions are Neumann-type boundary conditions. A current source of 1 A is launched from the bottom plane to the center conductor in the metal layer (shaded layer). In Fig. 3, we plot the smallest 426 eignevalues. A clear gap between the zero eigenvalues and the nonzero ones can be seen. In Table IV, we list the detailed eigenvalue number from the 420th eigenvalue to the 426th eigenvalue. A gap between the 424th eigenvalue and the 425th eigenvalue can be clearly seen. The largest eigenvalue of this example is 4.85693×10^{31}. Thus, the first 424 eigenvalues are essentially zero, which is also verified by computing the same structure with a large length unit. In Fig. 4(a), we show the electric field distribution in the transverse plane at 1 Hz simulated by the proposed method. In Fig. 4(b), we plot the electric field distribution simulated by a conventional full-wave FEM solver. Clearly, the proposed method produces an accurate electric field distribution, whereas the traditional solver breaks down. In addition, we checked the normal component of the electric field in the two dielectric layers above the ground plane. The normal component of the electric field in the layer having $\epsilon_r = 4$ is $|E| = 9.4638658694489792 \times 10^{16}$, whereas that in the layer having $\epsilon_r = 8$ is $|E| = 4.7466856099169584 \times 10^{16}$, the ratio of which shows excellent agreement with the analytical value which is 2.

The last example is a lossy structure. It is a solid copper wire of length 4 μm, width 3 μm, and height 3 μm. The conductivity is 5×10^7 S/m. We injected a 4 A current along the length of the copper wire. In Table V, we list the resistance simulated

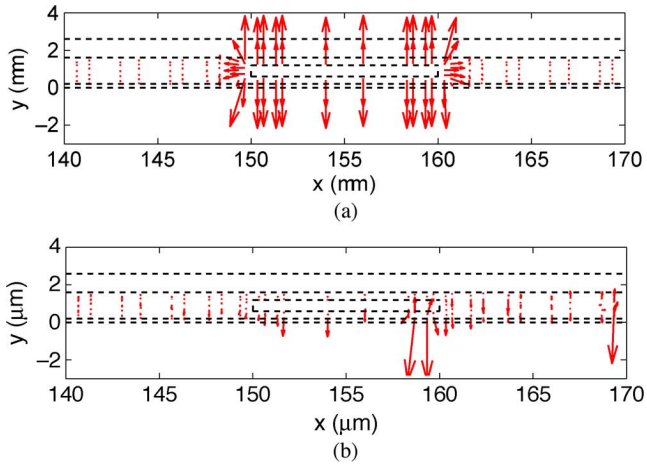

Fig. 4. (a) Electric field distribution generated by the proposed method. (b) Electric field distribution generated by a traditional full-wave FEM solver.

TABLE V
RESISTANCE SIMULATED BY THE PROPOSED METHOD (R) AND RESISTANCE SIMULATED BY THE TRADITIONAL FULL-WAVE FEM SOLVER (R^*)

Frequency (Hz)	R^* (Ω)	R (Ω)
1 K	0.008578164972632	0.008578164972632
10^{-6}	0.003484496898574	0.008578164972631
10^{-32}	$2.053771680135873 \times 10^{-53}$	0.008578164972631

by the conventional full-wave FEM solver, and that simulated by the proposed method at three low frequencies. Clearly, the conventional full-wave FEM solver for the lossy system inside conductors also breaks down at low frequencies, although the breakdown frequency is much lower than that of lossless cases. In contrast, the proposed method shows very good agreement with analytical resistance.

As pointed out at the end of Section III, each eigenmode has a different weight in the final field solution. The weight of the eigenmode that has a nonzero eigenvalue is orders of magnitude smaller than that of the dc mode at low frequencies. One thereby only needs to extract a reduced set of eigenvalues that are necessary for the frequency being considered. For the first example, we extracted only one eigenmode while the size of the matrix was 826. For the second example, 424 eigenvalues out of 1792 eigenvalues were used. The 424 eigenvalues are zero eigenvalues that include both physical dc mode and zero eigenvalues resulting from the null space of matrix $\mathbf{S}$ except that matrix T is replaced by R. For the third example, 41 eigenvalues out of 175 eigenvalues were used.

V. CONCLUSION

Full-wave FEM-based solutions break down at low frequencies. In this paper, we show that the low-frequency breakdown problem is caused by finite machine precision. Hence, this problem is associated with many electromagnetic applications. However, the problem is especially severe in VLSI circuit applications because the breakdown frequency is in the range of circuit operating frequencies.

To eliminate the low-frequency breakdown problem, first, one has to know what the actual solution of Maxwell's equations is at low frequencies. However, such a benchmark solution

does not exist because full-wave solvers break down at low frequencies while static solvers involve theoretical approximations. Hence, it is necessary to develop a theoretically rigorous method for solving Maxwell's equations at low frequencies. This paper provides for such a method. Furthermore, the method is equally applicable to high frequencies without any modification, and hence constituting a universal solution to Maxwell's equations in a full electromagnetic spectrum. The proposed method has been applied to the modeling of lossless and lossy VLSI circuits starting from dc. Numerical results have demonstrated its validity and rigor.

REFERENCES

[1] D. Jiao, C. Dai, S. Lee, T. Arabi, and G. Taylor, "Computational electromagnetics for high-frequency IC design," in *IEEE Int. Symp. Antennas Propag.*, 2004, vol. 3, pp. 3317–3320.

[2] D. Jiao, S. Chakravarty, and C. Dai, "A layered finite-element method for high-capacity electromagnetic analysis of high-frequency ICs," *IEEE Trans. Antennas Propag.*, vol. 55, no. 2, pp. 422–432, Feb. 2007.

[3] J. Lee, V. Balakrishnan, C. Koh, and D. Jiao, "A linear-time complex-valued eigenvalue solver for electromagnetic analysis of large-scale on-chip interconnect structures," *IEEE Trans. Microwave Theory Tech.*, vol. 57, no. 8, pp. 2021–2029, Aug. 2009.

[4] R. Dyczlj-Edllnger, G. Peng, and J. F. Lee, "Efficient finite element solvers for the Maxwell equations in the frequency domain," *Comput. Methods Appl. Mech. Eng.*, vol. 169, no. 3–4, pp. 297–309, Feb. 1999.

[5] S. C. Lee, J. F. Lee, and R. Lee, "Hierarchical vector finite elements for analyzing waveguiding structures," *IEEE Trans. Microwave Theory Tech.*, vol. 51, no. 8, pp. 1897–1905, Aug. 2003.

[6] S. Lee and J. Jin, "Application of the tree-cotree splitting for improving matrix conditioning in the full-wave finite-element analysis of high-speed circuits," *Microwave Optical Technol. Lett.*, vol. 50, no. 6, pp. 1476–1481, Jun. 2008.

[7] S. Lee, K. Mao, and J. Jin, "A complete finite element analysis of multilayer anisotropic transmission lines from DC to terahertz frequencies," *IEEE Trans. Adv. Packag.*, vol. 31, no. 2, pp. 326–338, May 2008.

[8] J. Zhu and D. Jiao, "A unified finite-element solution from zero frequency to microwave frequencies for full-wave modeling of large-scale three-dimensional on-chip interconnect structures," *IEEE Trans. Adv. Packag.*, vol. 31, no. 4, pp. 873–881, Nov. 2008.

[9] J. Zhu and D. Jiao, "Eliminating the low-frequency breakdown problem in 3-D full-wave finite-element-based analysis of integrated circuits," *IEEE Trans. Microwave Theory Tech.*, 2010, to be published.

[10] J. Zhao and W. C. Chew, "Integral equation solution of Maxwell's equations from zero frequency to microwave frequencies," *IEEE Trans. Antennas Propag.*, vol. 48, no. 10, pp. 1635–1645, Oct. 2000.

[11] A. Rong and A. C. Cangellaris, "Electromagnetic modeling of interconnects for mixed-signal integrated circuits from DC to multi-GHz frequencies," in *IEEE MTT-S Digest*, 2002, pp. 1893–1896.

[12] Y. Chu and W. C. Chew, "A surface integral equation method for solving complicated electrically small structures," in *IEEE 14th Topical Meeting Electrical Performance Electron. Packag. (EPEP)*, 2003, pp. 341–344.

[13] F. P. Andriulli, K. Cools, F. Olyslager, and E. Michielssen, "The "dot-trick TDEFIE": A DC stable integral equation for analyzing transient scattering from PEC bodies," in *IEEE Int. Symp. Antennas Propag.*, Jul. 2008, pp. 1–4.

[14] H. Bagci, F. P. Andriulli, F. Vipiana, G. Vecchi, and E. Michielssen, "A well-conditioned integral-equation formulation for transient analysis of low-frequency microelectronic devices," in *IEEE Int. Symp. Antennas Propag.*, Jul. 2008, pp. 1–4.

[15] L. Meirovitch, *Comutational Methods in Structural Dynamics*. Amsterdam, The Netherlands: Kluwer, 1980.

[16] D. J. Inman, *Vibration With Control, Measurement, and Stability*. Englewood Cliffs, NJ: Prentics-Hall, 1989.

[17] A. Preumont, *Vibration Control of Active Structures: An Introduction 2nd Eidition*. Amsterdam, The Netherlands: Kluwer, 2002, pp. 18–19.

[18] J. M. Jin, *The Finite Element Method in Electromagnetics*. New York: Wiley, 2002.

[19] A. Bossavit and I. Mayergoyz, "Edge-elements for scattering problems," *IEEE Trans. Magn.*, vol. 25, no. 4, pp. 2816–2821, Jul. 1989.

[20] J. Lee, V. Balakrishnan, C. Koh, and D. Jiao, "From $O(k^2N)$ to $O(N)$: A fast complex-valued eigenvalue solver for large-scale on-chip interconnect analysis," *IEEE Trans. Microwave Theory Tech.*, vol. 57, no. 12, pp. 3219–3228, Dec. 2009.

Jianfang Zhu (S'09) received the B.S. degree in electronic engineering and information science from University of Science and Technology of China, Hefei, China, in 2006, and is currently working toward the Ph.D. degree at Purdue University, West Lafayette, IN.

She now works in the On-Chip Electromagnetics Group, Purdue University, as a Research Assistant. Her current research interest is computational electromagnetics for large-scale high-frequency integrated circuit design.

Dan Jiao (S'00–M'02–SM'06) received the Ph.D. degree in electrical engineering from the University of Illinois at Urbana-Champaign, in 2001.

She then joined the Technology Computer-Aided Design (CAD) Division, Intel Corporation, until September 2005, as a Senior CAD Engineer, Staff Engineer, and Senior Staff Engineer. In September 2005, she joined Purdue University, West Lafayette, IN, as an Assistant Professor with the School of Electrical and Computer Engineering. In 2009, she was promoted to Associate Professor with tenure. She has authored two book chapters and over 100 papers in refereed journals and international conferences. Her current research interests include computational electromagnetics, high-frequency digital, analog, mixed-signal, and RF integrated circuit (IC) design and analysis, high-performance VLSI CAD, modeling of microscale and nanoscale circuits, applied electromagnetics, fast and high-capacity numerical methods, fast time-domain analysis, scattering and antenna analysis, RF, microwave, and millimeter-wave circuits, wireless communication, and bio-electromagnetics.

Dr. Jiao has served as the reviewer for many IEEE journals and conferences. She is an Associate Editor of the IEEE TRANSACTIONS ON ADVANCED PACKAGING. She was the recipient of the 2010 Ruth and Joel Spira Outstanding Teaching Award, the 2008 National Science Foundation (NSF) CAREER Award, the 2006 Jack and Cathie Kozik Faculty Start up Award (which recognizes an outstanding new faculty member of the School of Electrical and Computer Engineering, Purdue University), a 2006 Office of Naval Research (ONR) Award under the Young Investigator Program, the 2004 Best Paper Award presented at the Intel Corporation's annual corporate-wide technology conference (Design and Test Technology Conference) for her work on generic broadband model of high-speed circuits, the 2003 Intel Corporation's Logic Technology Development (LTD) Divisional Achievement Award in recognition of her work on the industry-leading BroadSpice modeling/simulation capability for designing high-speed microprocessors, packages, and circuit boards, the Intel Corporation's Technology CAD Divisional Achievement Award for the development of innovative full-wave solvers for high frequency IC design, the 2002 Intel Corporation's Components Research the Intel Hero Award (Intel-wide she was the tenth recipient) for the timely and accurate 2-D and 3-D full-wave simulations, the Intel Corporation's LTD Team Quality Award for her outstanding contribution to the development of the measurement capability and simulation tools for high frequency on-chip crosstalk, and the 2000 Raj Mittra Outstanding Research Award presented by the University of Illinois at Urbana-Champaign.